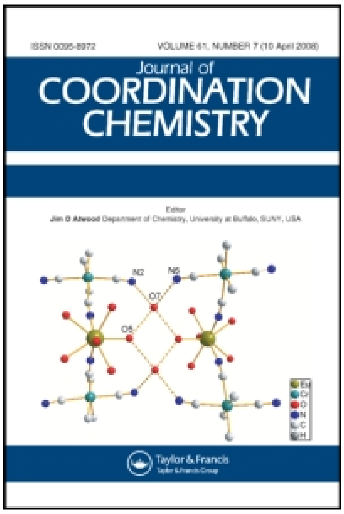

Journal of Coordination Chemistry
Publication details, including instructions for authors and subscription information:
http://www.informaworld.com/smpp/title~content=t713455674

Oxovanadium(IV) pyrazolyl carboxylic acid complexes: synthesis, crystal structures of $[VO(pzH)(HMPA)_2]_2 \cdot 4H_2O$ (1) and $VO(OH)(dmpzH)_2(C_6H_5COO)$ (2) (H_2MPA = 5-methyl-1*H*-pyrazole-3-carboxylic acid, pzH = pyrazole, dmpzH = 3,5-dimethyl pyrazole)

Zhang Peng Li[a]; Yong Heng Xing[a]; Yuan Hong Zhang[a]; Guang Hua Zhou[a]; Chun Guang Wang[a]; Jing Li[a]; Xiao Qing Zeng[b]; Mao Fa Ge[b]; Shu Yun Niu[a]
[a] Bioinorganic Laboratory, College of Chemistry and Chemical Engineering, Liaoning Normal University, Dalian, 116029, P.R. China [b] Institute of Chemistry, The Chinese Academy of Sciences, Beijing, 100080, P.R. China

To cite this Article Li, Zhang Peng , Xing, Yong Heng , Zhang, Yuan Hong , Zhou, Guang Hua , Wang, Chun Guang , Li, Jing , Zeng, Xiao Qing , Ge, Mao Fa and Niu, Shu Yun(2009) 'Oxovanadium(IV) pyrazolyl carboxylic acid complexes: synthesis, crystal structures of $[VO(pzH)(HMPA)_2]_2 \cdot 4H_2O$ (**1**) and $VO(OH)(dmpzH)_2(C_6H_5COO)$ (**2**) (H_2MPA = 5-methyl-1*H*-pyrazole-3-carboxylic acid, pzH = pyrazole, dmpzH = 3,5-dimethyl pyrazole)', Journal of Coordination Chemistry, 62: 4, 564 — 576, First published on: 01 October 2010 (iFirst)

To link to this Article: DOI: 10.1080/00958970802298402

URL: http://dx.doi.org/10.1080/00958970802298402

Journal of Coordination Chemistry
Vol. 62, No. 4, 20 February 2009, 564–576

Oxovanadium(IV) pyrazolyl carboxylic acid complexes: synthesis, crystal structures of $[VO(pzH)(HMPA)_2]_2 \cdot 4H_2O$ (1) and $VO(OH)(dmpzH)_2(C_6H_5COO)$ (2) (H_2MPA = 5-methyl-1*H*-pyrazole-3-carboxylic acid, pzH = pyrazole, dmpzH = 3,5-dimethyl pyrazole)

ZHANG PENG LI†, YONG HENG XING*†, YUAN HONG ZHANG†,
GUANG HUA ZHOU†, CHUN GUANG WANG†, JING LI†,
XIAO QING ZENG‡, MAO FA GE‡ and SHU YUN NIU†

†Bioinorganic Laboratory, College of Chemistry and Chemical Engineering,
Liaoning Normal University, Dalian, 116029, P.R. China
‡Institute of Chemistry, The Chinese Academy of Sciences, Beijing,
100080, P.R. China

(*Received 11 January 2008; in final form 30 April 2008*)

Two new monomeric complexes of oxovanadium(IV), $[VO(pzH)(HMPA)_2]_2 \cdot 4H_2O$ (**1**) and $VO(OH)(dmpzH)_2(C_6H_5COO)$ (**2**) (H_2MPA = 5-methyl-1*H*-pyrazole-3-carboxylic acid, pzH = pyrazole, dmpzH = 3,5-dimethyl pyrazole), have been synthesized from reaction of $VOSO_4 \cdot nH_2O$ with respective ligands. The compounds were characterized by elemental analysis, IR spectra and X-ray diffraction. Structural analysis of **1** and **2** gave the following parameters: **1**, monoclinic, $P2(1)/n$, $a = 11.1729(13)$ Å, $b = 23.965(3)$ Å, $c = 13.5591(15)$ Å, $\beta = 99.969(2)^\circ$, $V = 3575.8(7)$ Å^3, $Z = 4$; **2**, orthorhombic, *Pbcn*, $a = 13.197(4)$ Å, $b = 15.898(5)$ Å, $c = 18.192(6)$ Å, $V = 3817(2)$ Å^3, $Z = 8$. In each complex the vanadium is a distorted tetragonal bipyramid, which is typical for oxovanadium(IV) complexes. In both complexes, inter- and intra-molecular hydrogen bonds are also discussed. Complex **1** exists as an infinite chain along the b-axis by intermolecular hydrogen bonds. In addition, thermal analysis and quantum chemistry calculations were performed for analyzing the stability of the complexes.

Keywords: Oxovanadium(IV) complexes; Pyrazole ligand; Carboxylic acid; Hydrogen bonds; Crystal structures

1. Introduction

Coordination chemistry of vanadium has received more attention because of the activities of its compounds in various biological systems [1–3]. Vanadium compounds have the ability to lower plasma glucose levels, stimulate glucose uptake and glycogen synthesis [4, 5], and improve insulin sensitivity in a variety of animal models of both type I and type II diabetes [6–9]. Inorganic vanadyl cation (VO^{2+}) has therapeutic

---

*Corresponding author. Email: yhxing2000@yahoo.com

Journal of Coordination Chemistry
ISSN 0095-8972 print/ISSN 1029-0389 online
DOI: 10.1080/00958970802298402

effects as an insulin-mimetic [10], however, inorganic vanadium salts are poorly absorbed from the digestive system and have high toxicity.

Research has been directed towards the synthesis of efficient insulin-mimetic compounds with different ligands [9, 11]. In particular, pyrazole-based ligands have attracted interest because of monodentate, bridging bidentate, chelate, tridentate binding [12–14]. Our group has carried out investigation of oxovanadium complexes with polypyrazolyl ligands, such as $VO(O_2)(pzH)(HB(pz)_3)$, $VO(O_2)(pzH)(B(pz)_4)$ [15], $VO(HB(pz)_3)(H_2B(pz)_2)$, $VO(B(pz)_4)_2$ [16], $VO\{HB(pz)_3\}$(Me-acac), $VO\{HB(3,5\text{-}Me_2pz)_3\}$(Me-acac), $VO\{HB(pz)_3\}$(Et-acac), $VO\{HB(3,5\text{-}Me_2pz)_3\}$(Et-acac), etc. [17]. Vanadium complexes containing pyrazole, $V(pzH)_4Cl_2$, $V(pzH)_4Br_2$ and $V(pzH)_6Cl_2$, were reported by Larkworthy *et al.* [18]; Carrano *et al.* [19] reported the crystal structure of $[(Me_2pzH)_2VOCl_2]_2 \cdot THF$, and then reported the synthesis and structures of $[(pzH)_4VOCl]Cl \cdot H_2O$, $VOCl_2(3,5\text{-}Me_2pzH)_2(H_2O)$ and $[(t\text{-}BupzH)_4VO(H_2O)]Cl_2$ [20]. However, to our knowledge, oxovanadium-heterocyclic complexes with carboxylic acid ligands are rare. In this article we report the synthesis and crystal structures of two new oxovanadium complexes with heterocycles and carboxylic acid ligands: $[VO(pzH)(HMPA)_2]_2 \cdot 4H_2O$ (**1**) and $VO(OH)(dmpzH)_2(C_6H_5COO)$ (**2**) (H_2MPA = 5-methyl-1*H*-pyrazole-3-carboxylic acid, pzH = pyrazole, dmpzH = 3, 5-dimethyl pyrazole). Spectra, thermal decomposition and quantum chemistry calculations will be discussed.

2. Experimental

2.1. *Reagents and instrumentation*

All chemicals were of analytical grade and used without purification. H_2MPA was prepared by modified literature method [21] and all the other reactants were used as purchased. All synthetic manipulations were carried out in the atmosphere. IR spectra were recorded with a JASCO FT/IR-480 spectrometer (220–4000 cm^{-1}, with pressed KBr pellets). Elemental analyses (C, H, N) were performed on a PE 240C automatic analyzer.

2.2. *Synthesis*

2.2.1. Preparation of 5-methyl-1*H*-pyrazole-3-carboxylic acid

2.2.1.1. *5-methyl-1H-pyrazole-3-carboxylate.* To a solution of sodium ethoxide was added diethyl oxalate (0.50 mol) and acetone (0.50 mol), and the mixture was stirred at room temperature for 4 h. Then, acidified with acetic acid (0.50 mol), hydrazine hydrate (0.60 mol) was added and the mixture refluxed for 2 h. Pale yellow product was isolated by filtration and recrystallized from ethanol-water. Yield: 67.00 g, 86.90%. Anal. Calcd for $C_7H_{10}N_2O_2$: C, 54.54; H, 6.54; N, 18.17%. Found: C, 54.63; H, 6.66; N, 18.27%.

2.2.1.2. *5-methyl-1H-pyrazole-3-carboxylic acid.* A solution of 5-methyl-1*H*-pyrazole-3-carboxylate (7.70 g, 0.05 mol) and sodium hydroxide (4.80 g, 0.12 mol) in water

(300 mL) was heated under reflux for 5 h and then cooled to room temperature. Acidification with hydrochloric acid afforded H_2MPA as a white solid. Yield: 5.91 g, 94.00%. Anal. Calcd for $C_5H_6N_2O_2$: C, 47.62; H, 4.80; N, 22.21%. Found: C, 47.68; H, 4.96; N, 22.32%.

2.2.2. Preparation of complexes

2.2.2.1. *[VO(pzH)(HMPA)$_2$]$_2$·4H$_2$O (**1**).* 0.25 g (2 mmol) H_2MPA and 0.07 g (1 mmol) pyrazole were mixed in a Schlenk flask, 10 mL MeOH was added and the mixture was stirred for 15 min. Then solution of $VOSO_4 \cdot nH_2O$ (0.23 g, 71.00%, 1 mmol) in CH_3OH (5 mL) was added dropwise to the stirring mixture, and stirring continued for 4 h at room temperature to produce a cyan suspension. The precipitate was filtered out and the cyan filtrate stood at room temperature for several days giving violet-blue crystals suitable for X-ray diffraction. Yield: 0.37 g, 88.00% (based on V). Anal. Calcd for $C_{26}H_{36}N_{12}O_{14}V_2$: C, 37.06; H, 4.31; N, 19.95%. Found: C, 37.12; H, 4.27; N, 19.88%. IR (KBr, cm^{-1}): 3404($\nu_{O\text{–}H}$), 3137($\nu_{N\text{–}H}$), 1631($\nu_{asC=O}$), 1422($\nu_{sC=O}$), 965($\nu_{V=O}$), 792($\delta_{C\text{–}H}$), 472($\nu_{V\text{–}N}$), 388, 350($\nu_{V\text{–}O}$).

2.2.2.2. *VO(OH)(dmpzH)$_2$(C$_6$H$_5$COO) (**2**).* $VOSO_4 \cdot nH_2O$ (0.23 g, 71.00%, 1 mmol), dmpzH (0.18 g, 2 mmol), benzoic acid (0.12 g, 1 mmol) and KOH (0.06 g, 1 mmol) were dissolved in 10 mL MeOH/H_2O (1 : 1) and stirred at 70°C for 8 h to make a dark-green suspension. The precipitate was filtered out and the blue filtrate kept at room temperature for several days giving blue crystals suitable for X-ray diffraction. Yield: 0.12 g, 30.00% (based on V). Anal. Calcd for $C_{17}H_{22}N_4O_4V$: C, 51.39; H, 5.58; N, 14.10%. Found: C, 51.36; H, 5.56; N, 14.16%. IR (KBr, cm^{-1}): 3427($\nu_{O\text{–}H}$), 3132($\nu_{N\text{–}H}$), 1577($\nu_{asC=O}$), 1418($\nu_{sC=O}$), 945($\nu_{V=O}$), 793($\delta_{C\text{–}H}$), 455, 436($\nu_{V\text{–}N}$), 366, 338($\nu_{V\text{–}O}$).

2.3. *X-ray data collection and refinement of crystal structures*

Crystals of **1** and **2** were mounted on a glass fiber for X-ray measurement. Reflection data were collected at room temperature on a Bruker AXS SMART APEX II CCD diffractometer with graphite-monochromated Mo-Kα radiation ($\lambda = 0.7107$ Å) and ω-scan mode. All measured independent reflections were used in the structural analyses, and semi-empirical absorption corrections were applied using SADABS [22]. The crystal data, data collection, and refinement details are summarized in table 1.

The structures were solved by direct methods using SHELXS-86 and refined using SHELXTL-97 [23]. All non-hydrogen atoms were refined anisotropically and hydrogen atoms were included in calculated positions, constrained to ride on their carbon atoms with group U_{iso} values assigned. Atomic scattering factors and anomalous dispersion terms were as in SHELXTL-97. The drawings were made with Diamond [24] and all calculations were performed on a Pentium 4 computer.

2.4. *Thermogravimetric assay of 1 and 2*

Thermogravimetric analyses (TGA) were carried out on a Perkin-Elmer Diamond TG/DTA instrument. The samples are initially heated for 1 h at 50°C to remove air.

Table 1. Crystallographic data and structure refinement for **1** and **2**.

Formula	$C_{26}H_{36}N_{12}O_{14}V_2$	$C_{17}H_{22}N_4O_4V$
M (g mol^{-1})	842.55	397.33
Crystal system	Monoclinic	Orthorhombic
Space group	*P*2(1)/*n*	*Pbcn*
Unit cell dimension (Å, °)		
a	11.1729(13)	13.197(4)
b	23.965(3)	15.898(5)
c	13.5591(15)	18.192(6)
β	99.969(2)	
V (Å^3)	3575.8(7)	3817(2)
Z	4	8
D_{Calcd} (Mg m^{-3})	1.565	1.383
Crystal size (mm^3)	$0.36 \times 0.11 \times 0.07$	$0.10 \times 0.16 \times 0.20$
F(000)	1736	1656
μ(Mo-Kα) (cm^{-1})	0.605	0.549
θ (°)	1.75 – 24.06	2.01 – 29.07
Reflections collected	16436	23577
Independent reflections ($I > 2(I)$)	3294	3431
Parameters	487	235
$\Delta(\rho)$ (e Å^{-3})	0.538, −0.665	0.359, −0.487
Goodness-of-fit	1.035	1.031
R^a	0.0685(0.1224)^b	0.0440(0.0678)^b
$wR_2{}^a$	0.1733(0.1973)^b	0.1219(0.1382)^b

$^a R = \Sigma \| F_o| - |F_c\| / \Sigma |F_o|$, $wR_2 = [\Sigma(w(F_o^2 - F_c^2)^2 / [\Sigma(w(F_o^2)^2]^{1/2}$; $[F_o > 4\sigma(F_o)]$.
^{b}Based on all data.

During the simple ramping experiment, weight changes were recorded as a function of temperature for a 10°C min^{-1} temperature ramp between 50 and 1000°C for **1** and **2** in nitrogen environments. The mass of **1** and **2** are 2.077 mg and 2.895 mg, respectively.

3. Results and discussion

3.1. *Synthesis*

Complex **1** can be synthesized in MeOH at room temperature, while **2** was synthesized in MeOH/H_2O (1 : 1) at 70°C.

$$\mathrm{VOSO_4} \cdot n\mathrm{H_2O} + 2\mathrm{H_2MPA} + \mathrm{pzH} \xrightarrow[\text{Room temperature}]{\text{MeOH}} \mathbf{1}$$

$$\mathrm{VOSO_4} \cdot n\mathrm{H_2O} + \text{benzoic acid} + 2\mathrm{dmpzH} + \mathrm{KOH} \xrightarrow[70^{\circ}\mathrm{C}]{\mathrm{MeOH/H_2O}} \mathbf{2}$$

For **1**, the MeOH solution of $VOSO_4 \cdot nH_2O$ was added dropwise to MeOH solution of H_2MPA and pzH, while for **2**, all starting materials were added at the same time into a stirring solution of MeOH/H_2O. For **1**, the pH = 5, while for **2**, the KOH was added to control pH = 7. Attempt to synthesize **2** by reacting $VOSO_4 \cdot nH_2O$ with benzoic acid and dmpzH in methanol (as for **1**) failed, showing that pH is a key factor and that the coordination capability of H_2MPA is stronger than benzoic acid at pH = 5. The colors of **1** and **2** are violet-blue and blue, respectively, indicating vanadium +4 (usually, the color of vanadium(V) complexes is colorless or pale yellow). Complexes **1** and **2** are

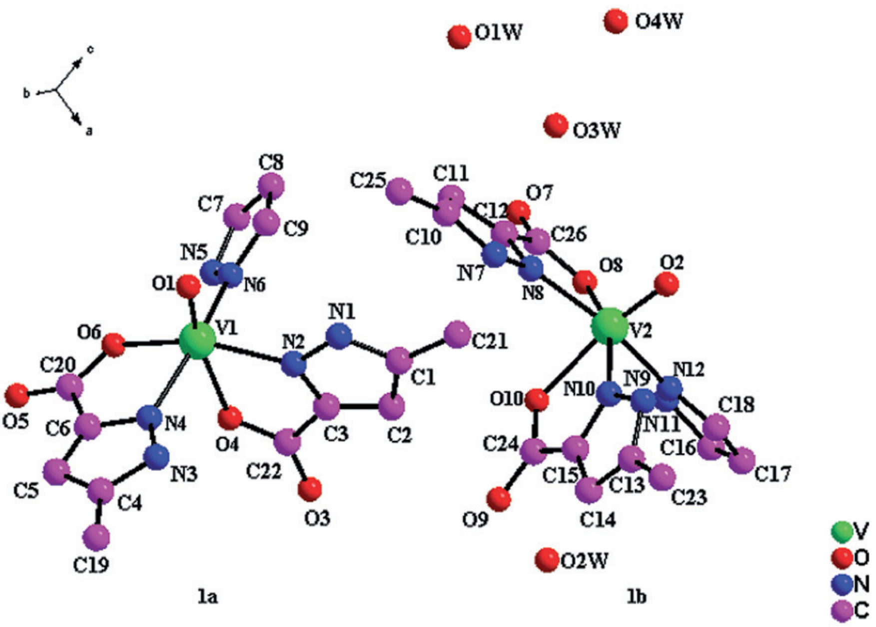

Figure 1. The crystal structure of **1** (hydrogen atoms are omitted for clarity).

stable in air (via IR spectra analysis and elemental analyses) and soluble in CH_2Cl_2, CH_3CN, THF, DMF, etc., insoluble in hexane and ether.

3.2. *IR spectra*

IR spectra of **1** and **2** show a broad band at 3400 cm^{-1} attributed to hydrogen bonds. For **1**, the asymmetric and symmetric stretching vibrations of the carboxylate anion are at 1631 cm^{-1} and 1422 cm^{-1}, respectively. The band at 965 cm^{-1} is characteristic of V=O. The $\nu_{V\text{–}N}$ is observed at 472 cm^{-1}. For **2**, the bands at 1577 cm^{-1} and 1418 cm^{-1} are attributed to asymmetric and symmetric stretching vibrations of the carboxylate, the V=O at 945 cm^{-1} and V–N stretching at 455 and 436 cm^{-1} [25, 26].

3.3. *Structural description*

3.3.1. $[VO(pzH)(HMPA)_2]_2 \cdot 4H_2O$ (1). As shown in figure 1, there are two independent molecules (**1a** and **1b**) and four lattice water molecules in an asymmetric unit. The vanadium in each molecule is six coordinate in a distorted tetragonal bipyramid defined by O1, O4, O6, N2, N4 and N6 for **1a** and O2, O8, O10, N8, N10 and N12 for **1b**. Axial sites are occupied by the oxo group (O1 for **1a** and O2 for **1b**) and an oxygen atom (O4 for **1a** and O10 for **1b**) from one HMPA. The equatorial plane is defined by the N2, N4, N6 and O6 for **1a**, and N8, N10, N12 and O8 for **1b**.

Selected bond distances and angles for **1** are listed in table 2. For **1a** the deviations from the least-squares plane containing the N2, N4, O6 and N6 atoms are 0.0709, –0.0838,

Table 2. Selected bond lengths (Å) and angles (°) for **1**.

1a							
V1–O1	1.583(4)	O6–V1–N4	78.30(17)	N4–V1–O4	97.8(2)	C22–O4–V1	118.5(4)
V1–O6	2.003(4)	N2–V1–N4	91.74(19)	O6–V1–N2	168.2(2)	C20–O6–V1	118.9(4)
V1–N6	2.098(5)	O6–V1–N6	85.86(18)	O1–V1–O4	158.25(19)	C3–N2–V1	118.1(4)
V1–N2	2.108(5)	N6–V1–N2	98.38(18)	O6–V1–O4	94.7(2)	N1–N2–V1	134.7(4)
V1–N4	1.997(4)	O1–V1–O6	83.52(17)	N6–V1–O4	107.0(2)	N3–N4–V1	140.4(4)
V1–O4	2.199(4)	O1–V1–N6	73.47(17)	N2–V1–O4	95.4(2)	C6–N4–V1	112.7(4)
		O1–V1–N2	84.79(16)	N6–V1–N4	87.04(18)	C9–N6–V1	127.6(4)
				O1–V1–N4	162.6(2)	N5–N6–V1	128.0(5)
1b							
V2–O2	1.584(4)	O8–V2–N8	85.81(17)	O2–V2–N12	161.2(2)	N7–N8–V2	141.2(4)
V2–O8	2.108(5)	N8–V2–N10	90.85(19)	N8–V2–N12	97.1(2)	C15–N10–V2	118.8(4)
V2–N8	2.091(5)	O8–V2–N12	87.56(19)	O2–V2–O10	159.76(18)	N9–N10–V2	134.8(4)
V2–O10	2.193(4)	N10–V2–N12	98.87(18)	O8–V2–N10	93.3(2)	C18–N12–V2	126.7(4)
V2–N12	2.109(5)	O2–V2–O8	81.53(19)	N8–V2–O10	77.74(17)	N11–N12–V2	127.2(5)
V2–N10	2.097(5)	O2–V2–N8	73.51(16)	N10–V2–O10	98.4(2)	C26–O8–V2	119.2(4)
		O2–V2–N10	86.30(16)	N12–V2–O10	106.95(19)	C24–O10–V2	118.0(4)
				O8–V2–O10	166.64(19)	C12–N8–V2	113.9(4)

0.0943 and −0.0814 Å, respectively, showing that these atoms are almost planar. V1, O1 and O4 lie −0.3041, −1.8794 and 1.8806 Å out of this plane, indicating that V1 lies toward the apical oxo group O1. The V1–O4 distance (2.199(4) Å) is longer than V1–O6 (2.098(5) Å) because O4 lies opposite to oxo group (O1) [27–29]. The V1–O6 and V1–O4 bond lengths are obviously longer than that of V1–O1, consistent with single bonds. Similarly, for **1b** the deviations from the least-square plane containing N8, N10, N12 and O8 are 0.0507, −0.0428, 0.0486 and −0.0565 Å, respectively. V2, O2 and O10 lie 0.3093, 1.8835 and −1.8677 Å out of this plane, respectively, indicating that V2 lies toward the apical oxo O2. The V2–O10 distance (2.193(4) Å) is longer than V2–O8 (2.108(5) Å) because O10 lies opposite to oxo [27–29]. There are four kinds of hydrogen bonds in **1**: (i) hydrogen bonds between the oxygen (donor) from lattice water and oxygen (acceptor) from carboxylate or the adjacent lattice water molecule: O1W–H1WA---O3#1 [#1: $x-1, y-1, z$], O1W–H1WA---O4, O2W–H2WB---O3#2 [#2: $-x+2, -y+1, -z+1$], O3W–H3WB---O1W, O4W–H4WA---O9#3 [#3: $x-1/2$, $-y+1/2$, $z+1/2$]; (ii) hydrogen bonds of the oxygen (donor) from lattice water with uncoordinated nitrogen (acceptor) from MPA: O3W–H3WA---N7; (iii) hydrogen bonds of uncoordinated nitrogen (donor) from MPA with the oxygen (acceptor) from carboxyl of a neighboring molecule: N1–H1B---O10#4, N3–H3A---O7#4 [#4: $-x+3/2, y+1/2, -z+3/2$], N7–H7A---O5#5, N9–H9A---O4#5 [#5: $x, y-1$, z]; (iv) hydrogen bonds of an uncoordinated nitrogen (donor) of pyrazole with oxygen (acceptor) from oxo of the adjacent molecule: N5–H5A---O2#6 [#6: $x, y+1, z$]. The D–H---A angles vary from 124.3(1)–168.1(6)°. Molecules of the mononuclear oxovanadium complexes are connected by intermolecular hydrogen bonds of N–H---O forming an infinite chain along the *b*-axis (figure 2). The length and angles of the hydrogen bonds are listed in table 3.

3.3.2. VO(OH)(dmpzH)$_2$(C$_6$H$_5$COO) (2). Structural analysis shows that in **2** the vanadium is a distorted tetragonal bipyramid. The terminal oxygen (O1) and the carboxylate oxygen (O3) from benzoic acid occupy the axial positions. One oxygen (O2)

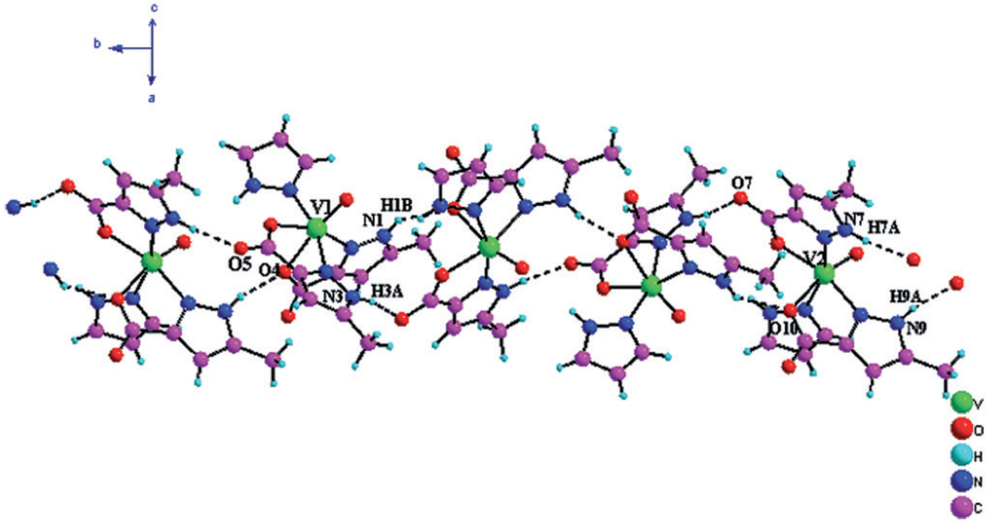

Figure 2. The hydrogen bonds of **1**.

Table 3. Bond lengths (Å) and angles (°) of hydrogen bonds in **1** and **2**.

D–H- - -A	d(D–H) (Å)	d(H ··· A) (Å)	d(D ··· A) (Å)	∠DHA (°)
Complex **1**				
O1W–H1WA- - -O4W	0.887(0)	2.568(7)	3.243(11)	133.4(3)
O3W–H3WB- - -O1W	0.805(9)	2.131(9)	2.832(9)	145.3(6)
O3W–H3WA- - -N7	0.833(1)	2.414(7)	3.208(7)	159.6(5)
O1W–H1WA- - -O3#1	0.887(0)	2.136(4)	2.737(6)	124.3(7)
O2W–H2WB- - -O3#2	0.838(2)	2.531(2)	3.182(9)	135.2(9)
O4W–H4WA- - -O9#3	0.830(3)	2.269(9)	2.853(11)	127.5(3)
N1–H1B- - -O10#4	0.860(3)	2.092(3)	2.844(6)	145.5(7)
N3–H3A- - -O7#4	0.860(7)	1.968(1)	2.783(6)	157.5(9)
N7–H7A- - -O5#5	0.859(2)	1.879(8)	2.735(6)	173.1(5)
N9–H9A- - -O4#5	0.859(5)	1.982(1)	2.829(6)	168.0(7)
N5–H5A- - -O2#6	0.860(7)	2.391(0)	3.203(8)	157.4(0)
Complex **2**				
O2–H2A- - -O3#7	0.820(0)	2.370(2)	3.157(1)	161.1(8)
N1–H1B- - -O2#7	0.859(7)	1.974(0)	2.821(1)	168.1(1)
N3–H3A- - -O3#7	0.860(7)	2.001(0)	2.854(1)	171.3(8)

Symmetry code: #1: $x-1, y-1, z$; #2: $-x+2, -y+1, -z+1$; #3: $x-1/2, -y+1/2, z+1/2$; #4: $-x+3/2, y+1/2, -z+3/2$; #5: $x, y-1, z$; #6: $x, 1+y, z$; #7: $-x, y, -z+1/2$.

from hydroxide, two nitrogens (N2, N4) from two 3,5-dimethylpyrazole ligands, and one oxygen (O4) from benzoic acid are in the equatorial plane. The structure and atomic labeling scheme for **2** are presented in figure 3.

The deviations of N2, O2, N4 and O4 atoms which compose the least-squares plane are 0.0289, −0.0289, 0.0279 and −0.0270 Å, respectively, showing that these atoms are almost planar. V, O1 and O3 lie 0.3882, 1.9909 and −1.8300 Å out of this plane, indicating that V lies toward the apical oxo O1. The V–O (O1, O2, O3 and O4) distances are 1.6043(16), 1.6268(16), 2.3898(16) and 2.1489(17) Å, respectively.

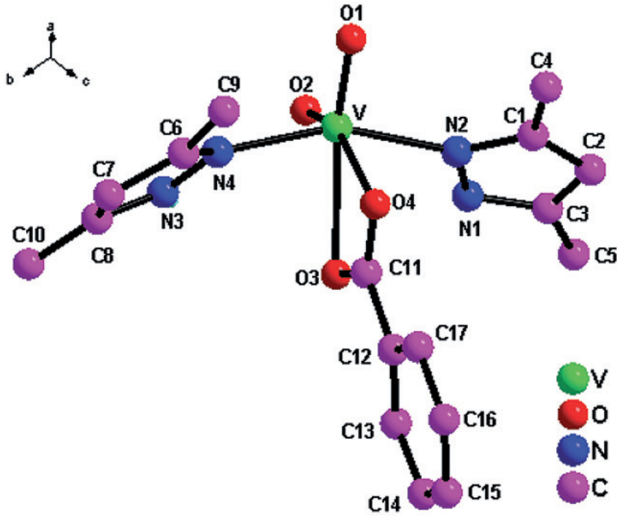

Figure 3. The crystal structure of **2** (hydrogen atoms are omitted for clarity).

Table 4. Selected bond lengths (Å) and angles (°) for **2**.

V–O1	1.6043(16)	O1–V–O2	107.47(9)	O2–V–O4	153.85(7)	O4–V–O3	57.02(5)
V–O2	1.6268(16)	O1–V–N4	99.72(8)	N4–V–O4	84.98(7)	C1–N2–V	97.34(13)
V–N4	2.0853(19)	O2–V–N4	92.86(8)	N2–V–O4	81.72(7)	N1–N2–V	86.40(12)
V–N2	2.0991(18)	O1–V–N2	99.63(8)	O1–V–O3	155.58(8)	C6–N4–V	132.85(15)
V–O4	2.1489(17)	O2–V–N2	91.39(8)	O2–V–O3	96.93(7)	N3–N4–V	120.11(12)
V–O3	2.3898(16)	N4–V–N2	157.92(7)	N4–V–O3	79.56(6)	C11–O3–V	135.55(16)
		O1–V–O4	98.57(8)	N2–V–O3	78.42(6)	C11–O4–V	118.83(13)

The distance from V to O3 (*trans* to the oxo group) is elongated compared to V–O4 due to *trans* influence of the oxo [27–29]. Selected bond distances and angles for **2** are listed in table 4.

In **2**, there are three types of intermolecular hydrogen bonds: N3–H3A---O3#7 (2.854(1) Å), O2–H2A---O3#7 (3.157(1) Å), N1–H1B---O2#7 (2.821(1) Å) [#7: $-x$, y, $\frac{1}{2}-z$]. The D–H---A angles in **2** vary from 161.1(8)–171.3(8)° and two adjacent molecules form a dimer by intermolecular hydrogen bonds (figure 4).

A comparison of the V–O bond lengths between **1** and **2** shows that V–O$_{\mathrm{trans}}$ (*trans* to terminal oxo) for **2** (2.389(8) Å) is longer than that of **1** (2.199(4) Å for **1a** and 2.193(4) Å for **1b**) because of different coordination modes of carboxylate, monodentate for **1** and bidentate for **2**. In addition, for **1**, the pyrazole with methyl substituted at position 5 increases oxygen electron density leading to a stronger V–O$_{\mathrm{carboxyl}}$. However, for **2**, coordinated carboxylate and benzene ring constitute a conjugated system, decreasing oxygen electron density leading to weaker V–O$_{\mathrm{carboxyl}}$. The V–O (terminal) double bond in **2** (1.6043(16) Å) is slightly longer than those of **1** (1.583(4) Å for **1a** and 1.583(4) Å for **1b**). The V–N average bond length for **1** (2.068(13) Å) is slightly shorter than that of **2** (2.092(2) Å), both of which are shorter than related oxovanadium complexes (table 5).

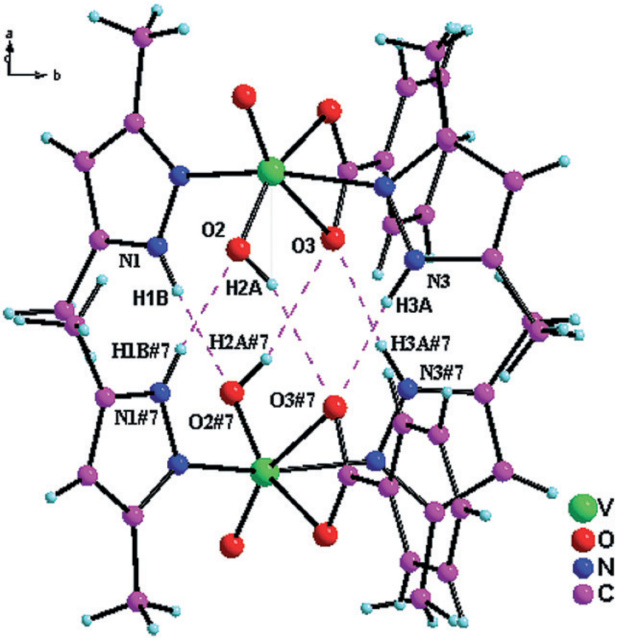

Figure 4. The hydrogen bonds of **2**.

Table 5. Comparison of some selected bond lengths (Å) for oxovanadium(IV) complexes.

Complex	V–O(terminal)	V–O(*trans*)	V–N(av)	Ref.
$[VO(pzH)(HMPA)_2]_2 \cdot 4H_2O$ (**1a**)	1.583(4)	2.199(4)	2.068(13)	This work
$VO(OH)(dmpzH)_2(C_6H_5COO)$ (**2**)	1.6043(16)	2.3898(16)	2.092(2)	This work
$[(dmpzH)_2VOCl_2]_2 \cdot THF$	1.591(13)	2.311(10)	2.129(11)	[19]
$VOCl_2(dmpzH)_2(H_2O)$	1.584(3)	2.268(3)	2.130(2)	[20]
$VOCl_2$(*t*-BupzH)$_4$$(H_2O)$	1.580(9)	2.136(9)	2.121(4)	[20]
$VO\{HB(pz)_3\}$(Me-acac)	1.590(5)		2.202(1)	[17]
$VO\{HB(dmpz)_3\}$(Me-acac)	1.597(2)		2.183(8)	[17]

t-BupzH: 3-*tert*-butylpyrazole.

Complex **2** contains a *cis*-$[V^{IV}O(OH)]^+$, which is identified in structurally characterized vanadium haloperoxidases and proposed as the active species in molybdoenzymes [30, 31]. Only a few compounds containing *cis*-$[V^{IV}O(OH)]^+$ core were isolated and characterized by X-ray single crystal diffraction, *cis*-$[V^{IV}O(OH)(bipy)_2][BF_4]$ (**3**), *cis*-$[V^{IV}O(OH)(phen)_2][BF_4] \cdot H_2O$ (**4**) and *cis*-$[V^{IV}O(OH)(4,4'\text{-dtbipy})_2]BF_4 \cdot 1.2H_2O$ (**5**) [30, 31]. The bond length of the V=O in **2** (1.6043(16) Å) is shorter than those in **3**, **4** and **5** (1.687(2), 1.677(3) and 1.659(6) Å, respectively) and V–OH in **2** (1.6268(16) Å) is shorter than those of the above complexes (1.761(2), 1.778(2) and 1.785(5) Å for **3**, **4** and **5**, respectively). The O–V–O angle of **2** (107.47(9)°) is similar to those of the above complexes (106.8(12)°, 106.35(12)° and 104.1(3)° for **3**, **4** and **5**, respectively).

Table 6. Frontier molecular orbitals eigenvalues (a.u.) in Hartree for **1** and **2**.

Orbital	HOMO-3	HOMO-2	HOMO-1	HOMO	LUMO
Complex **1**	−0.37588	−0.37502	−0.35824	−0.35777	0.09282
Complex **2**	−0.35414	−0.34797	−0.33353	−0.32974	0.10079

3.4. *Thermogravimetric analyses*

As shown in the Supplementary Material, thermal decomposition of **1** occurs in three steps. The first occurs within the temperature range 77–110°C with mass loss of 2.17% due to loss of water agreeing well with the theoretical weight loss (2.14%). The DTA curve of the complex indicates an endothermic process. The second stage of decomposition occurs within the temperature range 110–368°C with mass loss of 36.89% due to the loss of three water molecules and two 5-methyl-1*H*-pyrazole-3-carboxylic acid molecules agreeing with the theoretical weight loss (36.08%). The DTA curve shows an endothermic process. The third step with 29.68% (368–455°C) weight loss, corresponds to loss of two 5-methyl pyrazole-3-carboxylic acid molecules (29.67% theoretical weight loss). The DTA curve indicates an endothermic process.

The TG-DTG-DTA curves for **2** show two stages of thermal decomposition (Supplementary Material). The first occurs within the range 124–290°C with mass loss of 47.55% corresponding to loss of two 3,5-dimethyl pyrazole molecules (theoretical value 48.36%). The DTA curve indicates an endothermic process. The second stage from 410–520°C was observed as mass loss of 15.02% corresponding to loss of a half of benzoic acid molecule (theoretical value 15.30%). The DTA curve of the complex indicates an endothermic process.

3.5. *Electronic structure study*

We use Gaussian03W and MP2 method to investigate the electronic structure of **1** and **2**. A 6-31G* basis set is used for molecular system. The calculation included 39 and 48 atoms, 398 and 426 basis functions, 832 and 888 primitive Gaussians for **1** and **2**, respectively. The parameters of the molecular structures come from the crystal structure data. The electronic structures and the bonding of the complexes were analyzed with *ab initio* calculations and Natural Bonding Orbital analysis. The calculation gives the constitution and the energy of the molecular orbital and NBO atomic charge.

In general the stability of a complex is related to occupied orbitals, especially to the highest occupied orbital (HOMO). The energies of highest occupied molecular orbital of **1** and **2** are −0.35777 a.u. and −0.32974 a.u., the lowest unoccupied molecular orbital (LUMO) energy is 0.09282 a.u. and 0.10079 a.u., and the band gap is 0.45059 a.u. and 0.43053 a.u. (table 6).

The atomic net charges for the complexes calculated in the NBO analysis are listed in table 7. The valence of vanadium is +4, while the net charge of V is less than +4 (+2.16658 for **1** and +2.08599 for **2**), showing that the vanadium obtains some electron density from the ligands. For **1**, the net charges of O range from −0.95346 to −0.82670

Table 7. The atomic net charge for complex calculated at NBO analysis for **1** and **2**.

Atom	Complex **1**	Atom	Complex **2**
V1	2.16658	V	2.08599
O1	−0.82670	O1	−0.75254
O4	−0.95346	O2	−0.82468
O6	−0.93398	O3	−0.88755
N2	−0.49555	O4	−0.90498
N4	−0.46726	N2	−0.47031
N6	−0.43820	N4	−0.47571

Table 8. Selected Wiberg bond index and NBO bond order for **1**.

Bond	V1–O1	V1–O4	V1–O6	V1–N2	V1–N4	V1–N6
Wiberg bond index	1.7584	0.1491	0.2976	0.2087	0.2203	0.2194
NBO bond order	0.8866	0.1739	0.2766	0.2090	0.2124	0.2110

Table 9. Selected Wiberg bond index and NBO bond order for **2**.

Bond	V–O1	V–O2	V–O3	V–O4	V–N2	V–N4
Wiberg bond index	1.7633	1.6688	0.0885	0.1728	0.2628	0.2711
NBO bond order	0.8667	0.8336	0.0971	0.1726	0.2393	0.2453

and N range from −0.49555 to −0.43820. The net charge of O1 (−0.82670) is less negative than O4 (−0.95346) and O6 (−0.93398), and that of O4 is slightly different from O6 because of *trans* influence of terminal oxo group (O1) on O4. Similarly, for **2**, the net charges of O range from −0.90498 to −0.75254, and that of N2 (−0.47031) is close to N4 (−0.47571). Comparing the NBO bond order of **1** and **2** (tables 8 and 9) between metal and oxygen indicates that the vanadium oxygen bond from MPA is stronger than that from benzoic acid. In particular, for **2**, the Wiberg bond index of V−O1 and V−O2 are 1.7633 and 1.6688, respectively. The results are consistent with the structure analysis of **2**.

4. Conclusion

Two new oxo-V-pz-MPA and oxo-V-dmpz-BC (BC = benzoic acid, H_2MPA = 5-methyl pyrazole-3-carboxylic acid, pzH = pyrazole, dmpzH = 3,5-dimethyl pyrazole) complexes were synthesized and characterized by single crystal X-ray diffraction. The results of the X-ray structure analysis show that in **1** the carboxylate is monodentate, while that of **2** is bidentate. Complex **1** is the first example of an oxovanadium(IV) complex with simple pyrazole and pyrazolyl carboxylic acid. In addition, these studies have enriched the coordination chemistry of oxovanadium.

Supplementary material

Tables of atomic coordinates, isotropic thermal parameters, and complete bond distances and angles have been deposited with the Cambridge Crystallographic Data Center. Copies of this information may be obtained free of charge by quoting the publication citation and deposition numbers CCDC: 671866 for **1**, 671867 for **2**, from the Director, CCDC, 12 Union Road, Cambridge, CB2 1EZ, UK (Fax: +44–1223–336033; E-mail: deposit@ccdc.cam.ac.uk or http://www.ccdc.cam.ac.uk).

Acknowledgement

We wish to express our sincere thanks to the National Natural Science Foundation of China (Grant No. 20571036, 20771051).

References

[1] D.C. Crans, J.J. Smee, E. Gaidamauskas, L. Yang. *Chem. Rev.*, **104**, 849 (2004).

[2] M. Sutradhar, G. Mukherjee, M.G.B. Drew, S. Ghosh. *Inorg. Chem.*, **45**, 5150 (2006).

[3] N.S. Dean, L.M. Mokry, M.R. Bond, C.J. O'Connor, C.J. Carrano. *Inorg. Chem.*, **35**, 2818 (1996).

[4] M.Z. Mehdi, A.K. Srivastava. *Archives of Biochem. Biophys.*, **440**, 158 (2005).

[5] R.L. Khandelwal, S. Pugazhenthi. *Mol. Cell Biochem.*, **153**, 87 (1995).

[6] Y. Shechter, I. Goldwaser, M. Mironchik, M. Fridkin, D. Gefel. *Coord. Chem. Rev.*, **237**, 3 (2003).

[7] H. Sakurai, Y. Kojima, Y. Yoshikawa, K. Kawabe, H. Yasui. *Coord. Chem. Rev.*, **226**, 187 (2002).

[8] B.S. Parajón-Costa, O.E. Piro, R. Pis-Diez, E.E. Castellano, A.C. González-Baró. *Polyhedron*, **25**, 2920 (2006).

[9] R. Shukla, V. Barve, S. Padhye, R. Bhonde. *Bioorg. Med. Chem. Lett.*, **14**, 4961 (2004).

[10] R.A. Pederson, S. Ramanadham, A.M.J. Buchan, J.H. McNeill. *Diabetes*, **38**, 1390 (1989).

[11] M.T. Cocco, V. Onnis, G. Ponticelli, B. Meier, D. Rehder, E. Garribba, G. Micera. *J. Inorg. Biochem.*, **101**, 19 (2007).

[12] R. Mukherjee. *Coord. Chem. Rev.*, **203**, 151 (2000).

[13] G.B. Deacon, C.M. Forsyth, A. Gitlits, R. Harika, P.C. Junk, B.W. Skelton, A.H. White. *Angew. Chem. Int. Ed. Engl.*, **41**, 3249 (2002).

[14] M.F. Iskander, T.E. Khalil, W. Haase, R. Werner, I. Svoboda, H. Fuess. *Polyhedron*, **20**, 2787 (2001).

[15] Y.H. Xing, Y.H. Zhang, Z. Sun, L. Ye, Y.T. Xu, M.F. Ge, B.L. Zhang, S.Y. Niu. *J. Inorg. Biochem.*, **101**, 36 (2007).

[16] Y.H. Xing, B.L. Zhang, Y.H. Zhang, H.Q. Yuan, Z. Sun, M.F. Ge. *Polyhedron*, **26**, 3037 (2007).

[17] Y.H. Xing, K. Aoki, Z. Sun, M.F. Ge, S.Y. Niu. *J. Chem. Res.*, **2**, 100 (2007).

[18] L.F. Larkworthy, M.W. O'Donoghue. *Inorg Chim. Acta*, **71**, 81 (1983).

[19] E. Kime-Hunt, K. Spartalian, M. DeRusha, C.M. Nunn, C.J. Carrano. *Inorg. Chem.*, **28**, 4392 (1989).

[20] M. Mohan, M.R. Bond, T. Otieno, C.J. Carrano. *Inorg. Chem.*, **34**, 1233 (1995).

[21] J.D. Crane, O.D. Fox, E. Sinn. *J. Chem. Soc., Dalton Trans.*, 1461 (1999).

[22] G.M. Sheldrick. *SADABS, Program for Empirical Absorption Correction for Area Detector Data*, University of Göttingen, Göttingen, Germany (1996).

[23] G.M. Sheldrick. *SHELXS-86*, *Crystal Structure Solution Program*, Göttingen, Germany (1986); G.M. Sheldrick. *SHELXS-97*, *Program for Crystal Structure Refinement*, University of Göttingen, Göttingen, Germany (1997).

[24] K. Brandenburg, H. Putz. *Crystal and Molecular Structure Visualization Crystal Impact GbR*, Postfach 1251, D-53002, Bonn, Germany (2004).

[25] B.J.A. Jeragh, A. El-Dissouky. *Transition Met. Chem.*, **29**, 579 (2004).

[26] Y.H. Xing, Y.H. Zhang, Y.T. Xu, B.L. Zhang, S.Y. Niu, F.Y. Bai. *Chinese Science Bulletin*, **51**, 2189 (2006).

[27] D.C. Crans, A.D. Keramidas, S.S. Amin, O.P. Anderson, S.M. Miller. *J. Chem. Soc., Dalton Trans.*, 2799 (1997).

[28] K.K. Rajak, S. Mondal, S.P. Rath. *Polyhedron*, **19**, 931 (2000).

[29] N.S. Dean, M.R. Bond, C.J. O'Connor, C.J. Carrano. *Inorg. Chem.*, **35**, 7643 (1996).

[30] E.J. Tolis, M.J. Manos, A.J. Tasiopoulos, C.P. Raptopoulou, A. Terzis, M.P. Sigalas, Y. Deligiannakis, T.A. Kabanos. *Angew. Chem. Int. Ed.*, **41**, 2797 (2002).

[31] G.D. Triantafillou, E.I. Tolis, A. Terzis, Y. Deligiannakis, C.P. Raptopoulou, M.P. Sigalas, T.A. Kabanos. *Inorg. Chem.*, **43**, 79 (2004).